Observation of soft X-ray Cherenkov radiation in Al

SERGEY UGLOV[1(a)], ARTEM VUKOLOV[1], VALERY KAPLIN[1] , LEONID SUKHIKH[1] and PAVEL KARATAEV[2]

[1] *Tomsk Polytechnic University, Lenin Avenue 30, Tomsk 634050, Russia*
[2] *John Adams Institute at Royal Holloway, University of London, Egham, Surrey, TW20 0EX, UK*

received and accepted dates provided by the publisher
other relevant dates provided by the publisher

PACS 41.60.Bq – Cherenkov radiation
PACS 78.70.Dm – X-ray absorption spectra
PACS 41.60.Dk – Transition radiation

Abstract – The soft X-ray radiation generated by 5.7 MeV electrons from both an Al foil and a Mylar film in forward direction was experimentally studied. A narrow specific directivity, an ultra-narrow spectral bandwidth and a good consistency between the experiment and theory prove that the Cherenkov radiation (CR) with photon energy near the L-edge of absorption in Al was observed. The results demonstrate that the CR spectral-angular properties and the absolute photon yield can be described well enough using the Pafomov's theoretical model and the Henke's refractive index database, which is essential for all practical applications.

Introduction. - The Cherenkov radiation (CR) is generated by a fast charged particle in a medium with real part of the refractive index n (ω) > 1 in the light frequency, ω, range provided that the particle phase speed v > c/n(ω), where c is the speed of light in vacuum.

CR phenomenon in optical wavelength range is widely used in detectors of both photons and relativistic charged particles [1,2]. In a series of papers [3-5] CR in vacuum ultraviolet (VUV) spectral range has been represented as a mechanism to generate intense radiation suitable for practical application in, for example, lithography. It has been demonstrated both theoretically and experimentally that the CR spectral-angular density per single electron and at relatively low particle energies is a few orders of magnitude higher than that of the synchrotron radiation generated by much higher energy electrons [3-6].

For higher energies of emitted photons, for example, in soft X-ray (SXR) range the refractive index may exceed unity in a narrow spectral interval in the vicinity of K and L absorption edges of material atoms. Therefore one might expect that the CR generated in this spectral range has a very narrow spectral bandwidth Δω, being about 1 eV. The angular radiation density can be increased by an order of magnitude using shallow angles of particle incidence at the target surface [7,8].

The bottom line is that CR represents a promising, intense and highly monochromatic mechanism for SXR production. The source has a high potential for being used as a primary method for SXR radiation generation in compact accelerator based light sources, utilizing, for example, linear accelerator or betatron technologies with energies from 5 – 20 MeV [9-12], which is two orders of magnitude lower than modern synchrotron accelerator based central light source facilities.

A much higher intensity can be achieved via coherent emission, i.e. the longitudinal dimension of an ultra-short bunch is smaller than the CR wavelength, which can be achieved by a laser slicing or deliberately induced microbunching in the SXR wavelength range [13-15]. On the other hand, CR in SXR region can be used for transverse beam size and emittance diagnostics to reduce the diffraction limit [16, 17] and to minimise the effect of coherent radiation contribution [18-19] at, for example, an XFEL facility. So, due to the unique features of CR (directivity and monochromaticity) plus the fact that XFEL facilities have become available for users the need to investigate the CR phenomenon in SXR region has become obvious. Despite of the fact that the first experiment on CR observation in SXR range has been performed in 1981 [6], the mechanism was not well-investigated experimentally. There are only a few studies [6,7,9-12], in which an attempt to experimentally demonstrate CR in SXR range from solid targets was performed. Previously the effect of soft X-Ray Cherenkov Radiation (SXCR) was observed only from four elements: C (graphite), Si, V and Ti near *K* and *L* absorption edges. But for all that the authors of one paper [6] admit that they are not sure if they really observed SXCR due to large contribution of SXR from transition radiation (TR) and characteristic X-rays. In another paper [7] there is a significant discrepancy with theory. The lack of error-bars makes it impossible to evaluate the precision of those experiments. Moreover, there were negative experimental results for Ni. The results for the several carbon modifications (diamond, amorphous and

[(a)]E-mail: uglov@tpu.ru

polycrystalline graphite) [11] contradict with the first measurements presented in the paper [6]. Summarizing the past research and taking into account overall complexity of the experimental work in SXR spectral range there is an obvious need for further investigations of CR properties for other solid materials having $n > 1$ in SXR range before building instruments for practical applications. The most promising candidates around one hundred eV of photon energy are the targets made of Be, Si, and Al, because they have relatively high predicted CR photon yield and large radiation emission angle with respect to the electron beam trajectory [8,12]. In this Letter we present the results of the first experimental observation of the Cherenkov effect for Aluminium near the L- edge of photon absorption (E_{ch} = 72.6 eV) and their detailed comparison with theoretical predictions. For a crosscheck of the spectral properties of the radiation from the Al foil the results were compared with the properties of the radiation from a Mylar foil, for which the CR in the SXR range should be absent.

Theoretical calculations and the background contribution. – The theoretical estimation of the spectral range of SXCR from Al comes from Cherenkov condition $n(\omega) > 1/\beta$ and the equation of the dielectric permittivity $\varepsilon(\omega)$ (1)

$$\varepsilon(\omega) = 1 + \chi'(\omega) + i\chi''(\omega), \qquad (1)$$

where $\chi'(\omega)$ and $\chi''(\omega)$ are the real and imaginary parts of the electric susceptibility, $\beta = v/c$ is the speed of charged particle in units of the speed of light. Since $\varepsilon(\omega) = n^2(\omega)$, and $\chi'(\omega) << 1$ and $\chi''(\omega) << 1$ for SXR range, the condition $n(\omega) > 1/\beta$ corresponds to $\chi' > 0$ and, therefore, the CR condition can be interpreted as $\gamma^{-2} < \chi(\omega)'$, where γ is the Lorentz factor.

Figure 1a) illustrates the χ' and χ'' for Al near the L absorption edge taken from the database [20]. It is clear that $\chi' > 0$ stands for the photon energy range of E_{ph} = 64.2 – 96.6 eV. The filled area corresponds to the range of photon energies from 66.8 – 88.5 eV, where the condition $\gamma^{-2} < \chi'(\omega)$ is true. The medium atoms absorb the photons with energy above L absorption edge ($E > 72.6$ eV) where $\chi''(\omega)$ experiences a sharp jump. The area below L-edge energy is the effective CR area with E_{Ch} = 66.8 ÷ 72.6 eV marked in fig. 1a) by a darker color. For comparison, the χ' and χ'' susceptibilities for Mylar are shown as well by dashed lines. The $\chi' < 0$ across the entire spectral range shown, i.e. the CR cannot appear, whereas the transition radiation (XTR) in forward direction is still there. Due to the fact that forward XTR weakly depends on the target material properties, the comparison between Al and Mylar enables us to demonstrate the difference between SXCR and XTR.

The spectral-angular properties of SXR of TR and CR were calculated using the Pafomov's equations [21] for normal incidence of the electrons with total energy 5.7 MeV on the target surface excluding the effect of multiple scattering. The radiation spectrum ($dN/d\omega$) was obtained by integrating the spectral-angular distribution ($d^2N/(d\omega\, d\Omega)$) over all angles. The spectrum near the Al L absorption edge is characterized by a sharp asymmetric peak at $\hbar\omega$ = 72.6 eV, (see fig. 1b) – curve 1), standing on a broadband background given by TR contribution. Integrating the spectral distribution we have the CR yield $N = 3\cdot10^{-3}$ photon/electron. The green dash-dotted line represents the same calculations for Mylar. It is clear that only forward TR from an output surface is present.

To succeed in the experiment it was very important to evaluate the contribution of TR into the CR. From [21] the

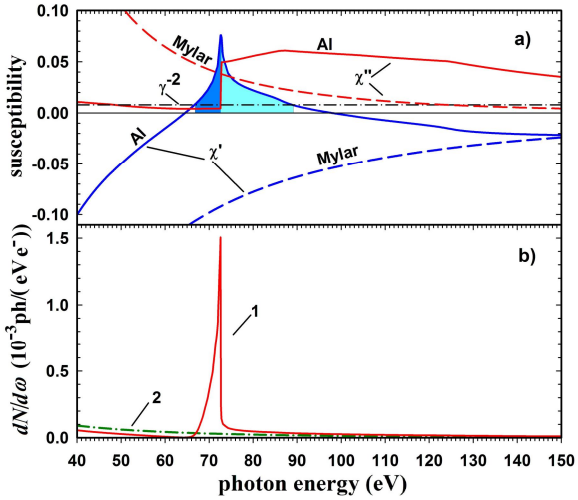

Fig. 1: (Colour on-line) a) The solid and dashed lines show the complex susceptibility around the L absorption edges for Al and Mylar, respectively, dash-dotted line indicates the Cherenkov threshold for 5.7 MeV electrons; b) The spectra of Cherenkov and transition radiations calculated with the Pafomov's theory [21] for Al (1) and Mylar (2).

TR and CR phenomena were calculated both independently and all together.

The angular distributions of TR, CR and their interplay integrated over the photon energy range from 30 – 200 eV are shown in fig. 2. One may see that the radiation intensity is largely dominated by TR with maximum emission angle of γ^{-1} corresponding to 5.1°. According to the theory the characteristic CR angle can be predicted using the formula $\cos(\theta_{Ch}) = 1/(\beta n(\omega))$ which can be approximated by $\theta_{Ch} = (\chi'(\omega) - \gamma^{-2})^{1/2} = 15.05°$ for $\chi'(\omega) << 1$ and $\gamma >> 1$. Despite of 3 times larger angle CR manifests itself as an extra high photon yield on top of TR angular distribution slightly broadening it. So, it is not useful to carry direct measurement of Al radiation angular distribution in the wide spectral range to establish the Cherenkov effect. However, thanks to high monochromaticity of CR in contrast to TR one could emphasize the CR effect measuring in a narrow spectral

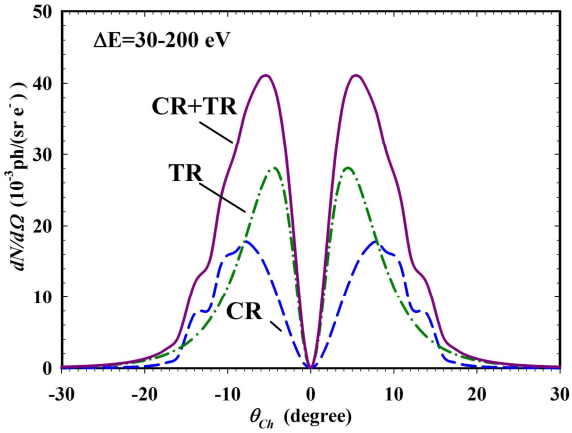

Fig. 2: (Colour on-line) The angular distributions integrated over energy range from 30 – 200 eV: TR – dashed-dotted line, CR – dashed line, and interplay of TR with CR – solid line. The calculations are performed for Al and 5.7 MeV electron energy.

range. This could be done using multilayer mirror as a Bragg reflection based monochromator in the spectral region of interest.

Method and setup. – The main challenge in this experiment is the apparatus configuration. The entire experimental station (including monochromator, manipulators, and detection hardware) must be sealed in vacuum. A schematic diagram of CR installation is illustrated in fig. 3, where θ_0 is the angle between the mirror surface and electron beam, θ_{Ch} is the emission angle

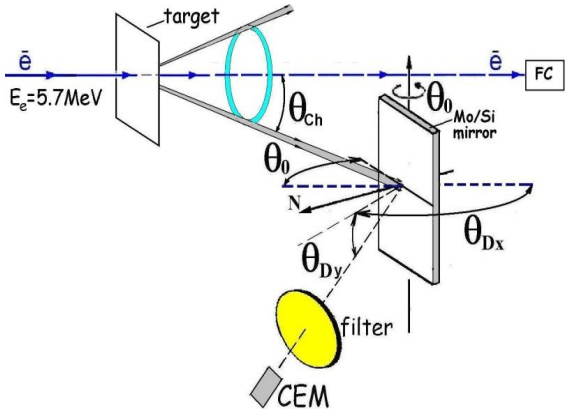

Fig. 3: (Colour on-line) Scheme for CR investigation using a multilayer mirror; CEM – detector of radiation, FC – Faraday cup.

of SXR from the target, $\theta_{Dy} = \theta_{Ch}$ and θ_{Dx} are the angles of the detection of radiation with a CEM (helix channel electron multiplier) detector. In order to demonstrate the detection of Cherenkov radiation the spectral composition of the radiation was investigated using Bragg reflection of radiation from a multilayer $[Mo/Si]_{50}$ mirror placed at a certain angle of emission. The rotation axis of the mirror coincides with the axis of the detector rotation and it is orthogonal to both the normal to the mirror surface and to the electron beam direction.

Figure 4 shows the calculation of the SXR CR and TR intensity reflected by the $[Mo/Si]_{50}$ mirror as a function of the mirror orientation angle θ_0 and direction of radiation emission set by θ_{Dy} for $\theta_{Dx}= 2\theta_0$ from the Al (a) and Mylar (b) targets. The theoretical calculations of the multilayer mirror reflectivity were performed using the formalism presented in [22]. The period of the $[Mo/Si]_{50}$ mirror consisting of 50 bi-layers was 11.32 nm. Due to the fact that the TR and CR are polarized in the emission plane, in the calculation of the final reflectance of the multilayer mirror, the division of radiation intensity into π and σ

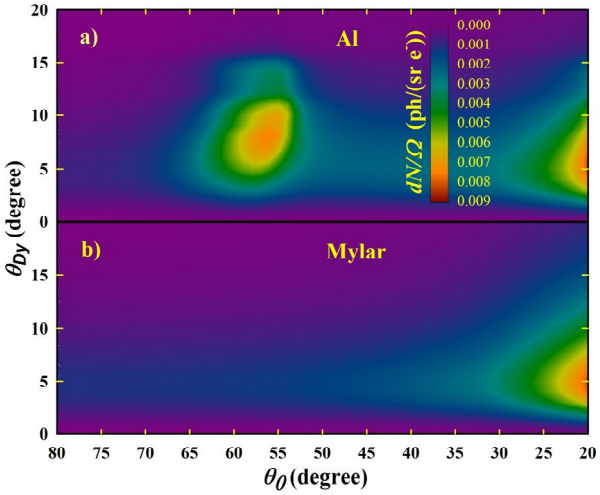

Fig. 4: (Colour on-line) Intensity of SXR reflected by multilayer $[Mo/Si]_{50}$ mirror vs angle θ_0 at an angle θ_{Dy}: a) Al, b) Mylar.

components ($I^{\parallel}$ and $I^{\perp}$) of polarization with respect to the mirror surface and the chosen direction of photon reflection was done using the expressions (2)

$$I_R^{\parallel} = I^{\parallel}\left(R_\pi \cos^2\psi + R_\sigma \sin^2\psi\right),$$
$$I_R^{\perp} = I^{\perp}\left(R_\pi \sin^2\psi + R_\sigma \cos^2\psi\right),$$
$$\cos\psi = \frac{[\vec{k}\times\vec{N}]}{|\vec{k}|}\frac{[\vec{k}\times\vec{V}]}{|\vec{k}||\vec{V}|}, \qquad (2)$$

where ψ is the angle between the plane of polarization of the emitted radiation defined by the wave vector ***k*** and the plane of radiation reflection from the mirror; ***V*** is the particle velocity and ***N*** is the normal to the mirror surface. Fig. 4a) shows a clear CR peak standing on a lengthy and weak TR background. In Fig 4(b) representing the same dependence for Mylar there is no peak where as the XTR background is present.

The experimental studies were carried out at the extracted beam of the M-5 microtron in the Tomsk Polytechnic University [23]. The basic beam parameters are summarized in table 1.

The $[Mo/Si]_{50}$ mirror with the area of 10 x 40 mm^2 was mounted on a goniometer in the center of the vacuum chamber and 200 mm away from a 9 μm thick Al target. The upper edge of the mirror was 20 mm below the electron beam trajectory.

Table 1: M-5 microtron electron beam parameters.

Beam energy, MeV	5.7
Beam repetition rate, Hz	25
Beam duration, μs	0.4
Single bunch population	$2.5 \cdot 10^7$
Single bunch length, ps	10
Bunch sequence frequency, GHz	2.8

The radiation was recorded by CEM detector model VEU – 6. The detector efficiency averaged over the input window (∅ – 9 mm) was $\xi = 6.9\%$ and 6.5% at the photon energies of E_{ph} = 96.7 and 77.1 eV, respectively. A set of permanent magnets was installed in front of the detector to protect it from scattered electrons. A 210 nm thick nitrocellulose filter was used to suppress soft TR component ($E < 30$ eV). The filter transmission for 72.6 eV photons was 0.06 [20]. The detector was 140 mm away from the mirror. A laser alignment system was used to set up the observation angles $\theta_{Dy} = 10°$ and 13° for Mylar and 10° and 18° for Al.

The angular acceptance of the detector was $\Delta\theta_{ch} = \pm$ 0.67°. The detector rotation axis coincided with the $[Mo/Si]_{50}$ mirror rotation axis. To determine the Bragg reflection, the radiation intensity was measured as a function of θ_{Dx} for each mirror orientation angle θ_0. The maximum was determined and used as a primary experimental value.

Result. – Figure 5 presents the measurements of radiation intensity at Bragg reflection as a function of θ_0 for Al and Mylar targets. The results presented by open and dark circles were obtained for the angle $\theta_{Dy} = 10°$. The results presented by squares and triangles were obtained for $\theta_{Dy} =$ 13° and 18°, respectively.

One may see that for Mylar the radiation is significantly lower than for Al at $\theta_{Dy} = 10°$. Moreover, the radiation quickly goes down when the multilayer mirror orientation angle changes. It suggests that the radiation is highly monochromatic. This is the property of the CR generated in the vicinity of the absorption edge.

The comparison of the calculated (fig. 4(a)) and experimental results for the Al target (fig. 5) shows that when $\theta_{Dy} = 10°$ both results have a peak radiation intensity with a maximum around $\theta_0 = 56°$. At the angles of radiation emission outside the Cherenkov cone $\theta_{Dy} > 15°$ both theoretical and experimental results have no singularities.

It should be noted that the lack of peculiarities in the experimental results for Al at the angles $\theta_{Dy} > 15$ ° indicates that we observed strongly-directed radiation and therefore the observed results cannot be explained by the contribution of characteristic radiation of L-series of Al (CXR), which is emitted isotropically. Furthermore, it indicates that the CXR contribution is very small. There is also a general agreement between the results of the calculations presented in fig. 4b) and the experimental results from the Mylar target. The intensity of TR radiation for both Al and Mylar are comparable and increases monotonically as a function of θ_0 as expected.

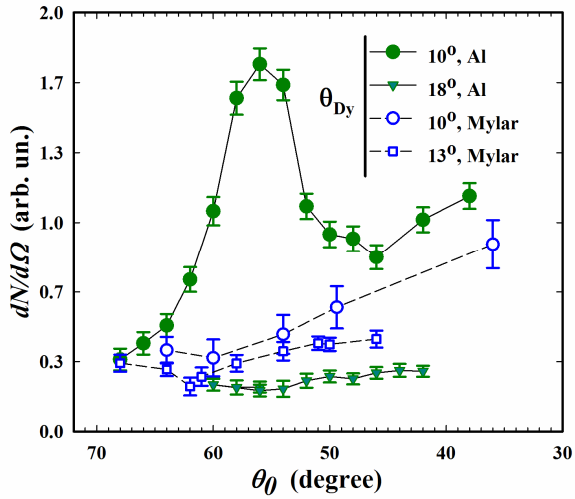

Fig. 5: (Colour on-line) Intensity of the reflected radiation as a functions of angle θ_0 of the $[Mo/Si]_{50}$ mirror for Al (dark circles and triangles) and Mylar (open circles and squares) targets; circles, squares and triangles are for $\theta_{Dy} =$ 10°, 13° and 18°, respectively.

Thus, the obtained results prove the observation of the Cherenkov effect in soft X-ray range.

Absolute photon yield. – For estimation of the absolute yield of SXCR a more detailed comparison of the experimental results with the model are presented in fig. 6.

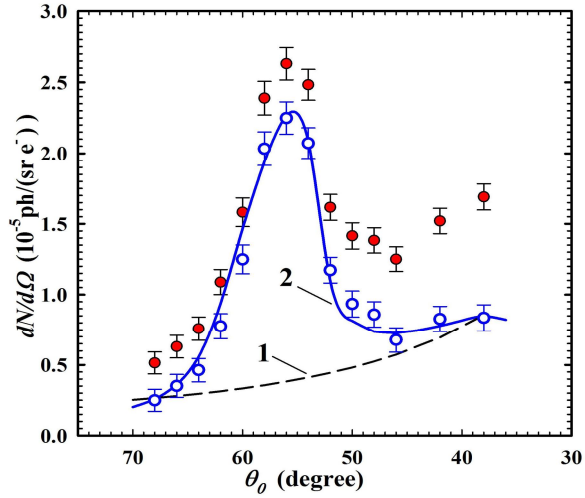

Fig. 6: (Colour on-line) Dark and open circles – measurements of radiation without and with subtraction of background, respectively; curve 1 – evaluated background; curve 2 – calculation accounting the detector efficiency $\xi = 0.063$ and the filter thickness of 0.21 μm.

The experimental results obtained at θ_{Dy} = 10° for the Al target are represented with dark circles. The solid line is the calculation. One may see that the calculated curve (fig. 6, solid line) and experimental points agree on the shape, but not quite on the absolute intensity. There is an additional background radiation increasing monotonically. The background can be explained by the luminescence appearing as a result of the direct interaction of electrons and bremsstrahlung with the multilayer mirror. The background is evaluated and presented in fig. 6 with a dashed line. If it is subtracted, the consistency of the theory and experiment is good.

Thus, the absolute intensity is 1.5 10^{-2} photons/(sr·e$^-$). Assuming that the systematic uncertainty of the absolute value determination is caused by the detection efficiency $\Delta\xi$ = 10% and the filter thickness Δt = 10%, the systematic uncertainty of radiation density measurement is 15%. The statistical uncertainty is much smaller than that.

Besides aluminium, Si, Mg or Be can also be used to generate CR with about 100 eV photon energy. The calculation of the angular density of CR generated by electrons with energy of 5.7 MeV from a semi-infinite target for all four elements is presented in fig.7, where the angular cone is divided into four sectors, each of which corresponds to a certain element. Table 2 summarises the basic parameters including brightness (in units of photons per electron and per unit solid angle).

Table 2: Specific yields of Cherenkov emitters.

	Mg	Al	Si	Be
E, eV	49.5	72.6	99.8	111.5
dE, eV	1.1	1.3	1.0	0.3
$dN/d\Omega_{max}$, ph/(e$^-$sr) 10^{-2}	3.1	2.03	1.14	1.66
Yield, ph/e$^-$ 10^{-3}	4.64	3.24	1.04	1.53

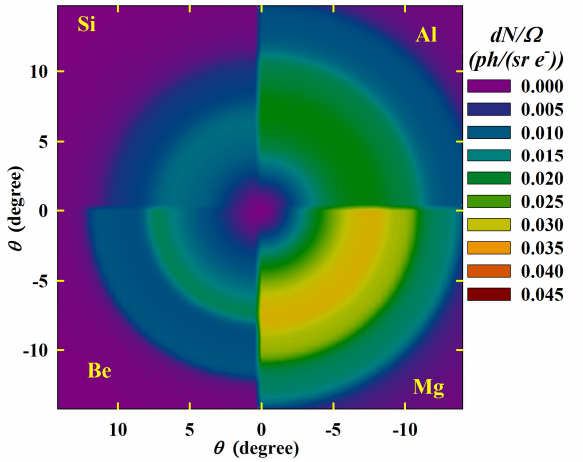

Fig. 7: (Colour on-line) The quarters of the angular distribution of CR for elements: Si, Al, Be, and Mg.

The 2D patterns shown in fig. 7 clearly demonstrate and allow one to compare the distribution of the whole angular density of CR for all four elements.

Comparing the emissivity of Al and Si radiators one should note that in case of an Al target the yield per single electron is a factor of 3 larger than for Si. The CR intensity is controlled by the number of electrons in a beam. However, increasing the beam population we increase the integral energy deposited in the target sample heating it. In practice the melting point T_m of the target material determines the maximum allowable temperature rise. The Al melting point (T_m=933° K) is relatively low in comparison with Si (T_m=1687° K). So if we take into account the target heating by the particle beam applying the method presented in [12], the maximum achievable yield for Al is more than 10 times lower than for Si. To resolve the problem one may foresee a cooling system to take the heat away and increase the electron beam intensity. On the other hand, if a limited intensity electron beam was used, an Al target would certainly be preferential.

Conclusion. – The primary purpose of this work was to observe the CR radiation from Al, measure its spatial spectral characteristics and absolute photon yield, and compare with the theoretical expectation. We have achieved convincing prove the observation of the soft X-Ray Cherenkov radiation generated by relativistic electrons in Al. The radiation intensity and spectral properties are in a good agreement with theoretical calculations performed using the theory [21] and the modern refractive index data for Al taken from Henke database [20]. Thanks to this experiment, the number of spectral lines generated due to Cherenkov mechanism in SXR region and consisting of highly monochromatic, intense, and experimentally confirmed peaks of V, Ti and Si *L*-edges of absorption is topped-up with the *L*-line of Al with energy of 72.6 eV.

Observation of CR form Al allows to start detailed investigation of the feasibility of this radiation for practical purposes that may include both radiation source based on a compact accelerator or new radiation source for transverse beam profile diagnostics in the extreme ultraviolet region [16].

***

This work has been supported by the Russian Foundation for Basic Research (project No. 14-02-01032), by the Program of Russian Ministry of Education and Science "Nauka", by the Federal Targeted Program of the Russian Federation (agreement #14.578.21.0198) and the Leverhulme Trust through the international Network Grant (IN-2015-012).

REFERENCES

[1] JELLEY J.V., *Cherenkov Radiation and Its Applications,* (Pergamon Press*)* 1958, p. 334.
[2] ANDRESEN R.D., ARENS I., TAYLOR B.G., WILLS R.D., *Nuclear Instruments and Methods,* **120** (1974) 85.

[3] PIESTRUP M. A., PANTELL R. H., PUTHOFF H. E., AND ROTHBART G. B., *Journal of Applied Physics,* **44** (1973) 5160.
[4] PIESTRUP M. A., POWELL R. A., ROTHBART G. B., CHEN C. K., AND PANTELL R. H., *Applied Physics Letters,* **28** (1976) 92.
[5] GOLOVIZNIN V.V., OEPTS D., VAN DER WIEL M.J., *Nuclear Instruments and Methods in Physics Research A*, **393** (1997) 510-5131.
[6] BAZYLEV V.A. *et al., Sov. Phys. JETP*, **54** (1981) 884.
[7] MORAN M. J., CHANG B., SCHNEIDER M. B., MARUYAMA X. K., *Nucl. Instrum. Methods Phys. Res., Sec. B*, 48 (1990) 287.
[8] GARY C., KAPLIN V., KUBANKIN A., NASONOV N., PIESTRUP M., UGLOV S., *Nuclear Instruments and Methods in Physics Research B*, **227** (2005) 95.
[9] KNULST W., LUITEN O. J., VAN DER WIEL M. J., AND VERHOEVEN J., *Appl. Phys. Lett.,* **79** (2001) 2999.
[10] KNULST W., VAN DER WIEL M. J., LUITEN, O. J. AND VERHOEVEN J., *Appl. Phys. Lett.*, **83** (2003) 4050.
[11] KNULST W., LUITEN J., VERHOEVEN J., *EEE Journal on Selected Topics in Quantum Electronics*, **10** (2004) 1414.
[12] KNULST W., *Ph.D. thesis,* Thechnische Universit, Eindhoven 2004.
[13] ROSENZWEIG J., TRAVISH G., TREMAINE A., *Nucl. Instr. and Meth. A,* **365** (1995) 255.
[14] GAZAZIAN E. D., ISPIRIAN K. A., ISPIRIAN R. K., IVANIAN M. I., *Pisma Zh. v Eksp. Teor. Fiz.*, **70** (1999) 664.
GAZAZIAN E. D., ISPIRIAN K. A., ISPIRIAN R. K., IVANIAN M. I., *Nucl. Instr. and Meth. B,* 173 (2001) 160.
[15] AGINIAN M. A., ISPIRIAN K. A., ISPIRYAN M. K., IVANYAN M. I., *Journal of Physics: Conference Series* **517** (2014) 012040.
[16] SUKHIKH L. G., KUBE G., BAJT S., LAUTH W., POPOV YU. A. AND POTYLITSYN A. P., *Phys. Rev. ST Accel. Beams*, **17** (2014) 112805.
[17] KONKOV A., KARATAEV P., POTYLITSYN A. AND GOGOLEV A., *Journal of Physics: Conference Series,* **517** (2014) 012003.
[18] WESCH S., BEHRENS C., SCHMIDT B., AND SCHMÜSER P., *in Proceedings of the 31st International Free Electron Laser Conference (FEL 09), Liverpool, UK, 2009, (STFC Daresbury Laboratory, Warrington) 2009,* p. 619.
[19] LOOS H., *in Proceedings of the Third International Beam Instrumentation Conference*, *Monterey, CA, 2014*, p. WEIXB1.
[20] *ftp://ftp.esrf.fr/pub/scisoft/DabaxFiles/f1f2_Henke.dat*
[21] PAFOMOV V. E., *Trudy FIAN*, **44** (1969) 28 [in Russian].
[22] PARRATT L. G., *Physical Review*, **95** (1954) 359.
[23] UGLOV S. R., KAPLIN V. V. *et al., J. Phys. Conf. Ser.,* **517** (2014) 012009.